

# LIMNOLOGY AND OCEANOGRAPHY

November 1999

Volume 44

Number 7

*Limnol. Oceanogr.*, 44(7), 1999, 1599–1608  
© 1999, by the American Society of Limnology and Oceanography, Inc.

## Implications of bio-optical modeling of phytoplankton photosynthesis in Antarctic waters: Further evidence of no light limitation in the Bransfield Strait

*Francisco G. Figueiras and Belén Arbones*

Instituto de Investigaciones Mariñas, CSIC, Eduardo Cabello 6, 36208 Vigo, Spain

*Marta Estrada*

Institut de Ciències del Mar, CSIC, P. Joan de Borbó s/n, 08039 Barcelona, Spain

### *Abstract*

During the cruise ECOANTAR 94 photosynthesis versus irradiance relationships, phytoplankton spectral absorption, quantum yield of carbon fixation, and water column light regime were determined in the eastern Bransfield Strait and surrounding areas of the Weddell Sea and Weddell–Scotia Confluence, to determine if photosynthesis is light limited in these areas. There were no significant differences in the light-saturated chlorophyll-specific rate of photosynthesis ( $P_m^B$ ), light-limited slope ( $\alpha^B$ ), light saturation parameter ( $E_{kPAR}$ ), and the maximum quantum yield ( $\phi_m$ ) between surface and subsurface water for several water masses in the area, which indicates that the photosynthetic response in the upper mixed layer was uniform. There were also no significant differences between the spectral light saturation parameter ( $E_{kPUR}$ ) and the mean absorbed irradiance by phytoplankton in the upper mixed layer ( $E_{umIPUR}$ ). These similarities suggest that phytoplankton photosynthesis was not light limited in this Antarctic region during the cruise period. This was also affirmed by the fact that the average operational quantum yield of the water column ( $0.03 \text{ mol C [mol photons]}^{-1}$ ) was half of the mean maximum quantum yield ( $0.06 \text{ mol C [mol photons]}^{-1}$ ). Primary production is underestimated by 24% when broadband models are compared with spectral ones. These results have important implications for the modeling of carbon flows in the Southern Ocean.

Research in the Southern Ocean has generated a sizeable database on rates of algal growth, primary production and phytoplankton distribution (e.g., El-Sayed 1970; Holm-Hansen et al. 1977; Figueiras et al. 1994). In general, most of the Antarctic waters are characterized by low to moderate productivity and low phytoplankton standing stocks. However, dramatic spatial and temporal variability occurs along the continental shelf and the ice-edge regions of the Weddell and Ross seas. In open Antarctic waters inorganic nutrient concentrations are very high but phytoplankton biomass is low. This scenario has been termed the biological paradox of the Southern Ocean (El-Sayed 1987) and has been attributed to the control imposed by low light levels in the well-mixed surface waters (Sakshaug and Holm-Hansen 1984), iron deficiency (Martin et al. 1991), and grazing (Smetacek et al. 1990).

### *Acknowledgements*

We thank all those who took part in the ECOANTAR 94 expedition on board R/V *BIO Hespérides*. We also thank G. H. Tilstone for useful criticisms of the manuscript. This research was supported by the CICYT (Spanish Commission of Science and Technology) projects ANT93–0997 and AMB93–0129. The work of B.A. was funded by a grant from Xunta de Galicia.

More recently it has been suggested that Antarctic phytoplankton in the upper mixed surface layer might not be light limited close to the ice-edge (Figueiras et al. 1994), around Elephant Island (Helbling et al. 1995) and in Bransfield and Weddell–Scotia waters (Figueiras et al. 1998). This suggestion came from the similarity found between the broadband light saturation parameter ( $E_{kPAR}$ ) and the mean PAR irradiance ( $E_{umIPAR}$ ) received by phytoplankton in the upper mixed layer, which indicates that phytoplankton is acclimated to the light regime in the water column. These works, however, did not consider the influence of the spectral light field on photosynthesis and primary production. It is well known that the spectral quality of light in the sea is susceptible to changes with depth, water quality, and the nature of the incident solar radiation, which in turn influences the absorption and utilization of light by phytoplankton (Kirk 1983). Hence, models of primary production that ignore the wavelength dependency potentially incur errors, although these are often used for simplicity. The determination of the photosynthetic action spectrum of carbon fixation by using spectral photosynthesis–irradiance relationships is time-consuming, expensive, and difficult to apply at sea and therefore few data of this nature are available. Re-

cently Kyewalyanga et al. (1997) and Arbones et al. (in prep.) have shown how to determine the action spectra and maximum quantum yields of carbon fixation of natural phytoplankton populations using white-light photosynthesis–irradiance relationships with a correction for the spectral dependency of photosynthesis. Briefly, these methods consist of correcting the spectral output of the light sources used in the photosynthesis–irradiance determinations, which are strongly biased toward the red end of the spectrum, by using the phytoplankton absorption coefficients.

This research presents results obtained from the eastern basin of the Bransfield Strait during the summer of 1994 on spectrally dependent photosynthesis–irradiance parameters. The spectral photosynthetic parameters are used to investigate light limitation of Antarctic phytoplankton in the deeply mixed surface waters and complements a previous study (Figueiras et al. 1998) in which no light limitation was deduced from total photosynthetically active radiation (PAR) and nonspectral photosynthetic parameters. Depth integrated primary production computed using the spectral light field and phytoplankton absorption is compared with primary production estimated using PAR irradiance.

## Methods

Between 9 and 31 January 1994 the eastern basin of the Bransfield Strait and the surrounding areas of the Weddell Sea and Drake Passage were sampled at 110 stations by R/V *Hespérides* (Fig. 1). Most of the stations were distributed in a dense grid covering the eastern basin of the Bransfield Strait, with eight stations located within the Drake Passage, northwest of the King George–Elephant Island line. Typically the internal Rossby radius of deformation in this region is around 30 km (García et al. 1994), and therefore, the distance between adjacent stations in the grid was established at approximately 15 km in order to resolve mesoscale aspects of the flow and to describe the hydrography. The melting waters of the pack ice-edge, which was found at the southeastern part of the sampling area, were also sampled at seven stations. Two long eastern transects were sampled from the ice-edge in the northwestern Weddell Sea to Drake Passage.

Bio-optical sampling was conducted at 23 stations uniformly distributed along the sampling region (large dark circles in Fig. 1). An initial conductivity–temperature–depth (CTD)–fluorescence profile was performed at all stations with an EG&F MkIIIc WOCE and rosette. Two depths were sampled at each bio-optical station. Surface (5–10 m) and 50 m depth were sampled at stations with a homogeneous profile of fluorescence in the surface layer (see for example Stas. 119 and 102 in Fig. 2). When a subsurface chlorophyll maximum was observed in the CTD–fluorescence profiles (e.g., Stas. 63 and 13 in Fig. 2), usually between 30 and 70 m, depths corresponding to the subsurface maximum were sampled instead of 50 m. Water samples were collected during the upcast using 12 liters PVC Niskin bottles from the rosette.

*Light in the water column*—Profiles of photosynthetically active radiation (PAR) were measured at 5–10-m intervals

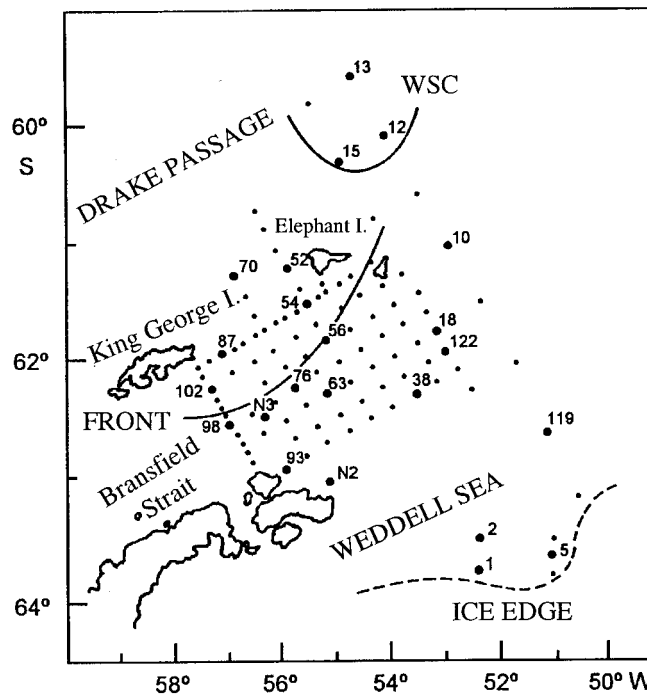


Fig. 1. Chart of the sampling area showing the positions of CTD stations. The numbered larger circles correspond to the stations where bio-optical sampling was done. The location of the three main hydrographic features is shown: Ice-Edge; WSC, Weddell–Scotia Confluence; FRONT is the frontal structure that separates Bransfield waters with influence of Bellingshausen Sea (northern area) from Bransfield waters with influence of Weddell Sea.

at each bio-optical station with a Li-Cor spherical quantum sensor LI193SA. The irradiance at the sea surface was monitored on deck with a Li-Cor cosine-corrected LI-190SA sensor taking readings at minute intervals that were integrated every 10 min. Because of the frequent and rapid pass of cloud fronts in Antarctica that can cause high short-time variability in irradiance, this was averaged to obtain the mean of the daily incoming irradiance at the sea surface ( $\overline{E_{0+}}$ ). In this way, the short variability that can preclude any generalization of the results was removed. The average daily irradiance just below the sea surface ( $\overline{E_{0-}}$ ) was estimated from  $\overline{E_{0+}}$ , considering 0.8 as the transmittance at the air–sea interface (Austin 1974).

The spectral irradiance in the water column was determined at 5–10-m intervals with an Li-1800 spectroradiometer. The monthly average daily spectrum of the irradiance just below the sea surface,  $\overline{E_{0-}}(\lambda)$ , was estimated from the mean of the spectra at 0 m normalized to the integral of this mean spectrum and multiplied by the mean PAR irradiance just below the sea surface:

$$\overline{E_{0-}}(\lambda) = \overline{E_{0-}} \cdot \overline{E_{0-}}(\lambda) / \int_{\lambda} \overline{E_{0-}}(\lambda) d\lambda \quad (1)$$

The mean PAR irradiance ( $E_{umlPAR}$ ) received by phytoplankton moving in the upper mixed layer ( $Z_{uml}$ ) was estimated as

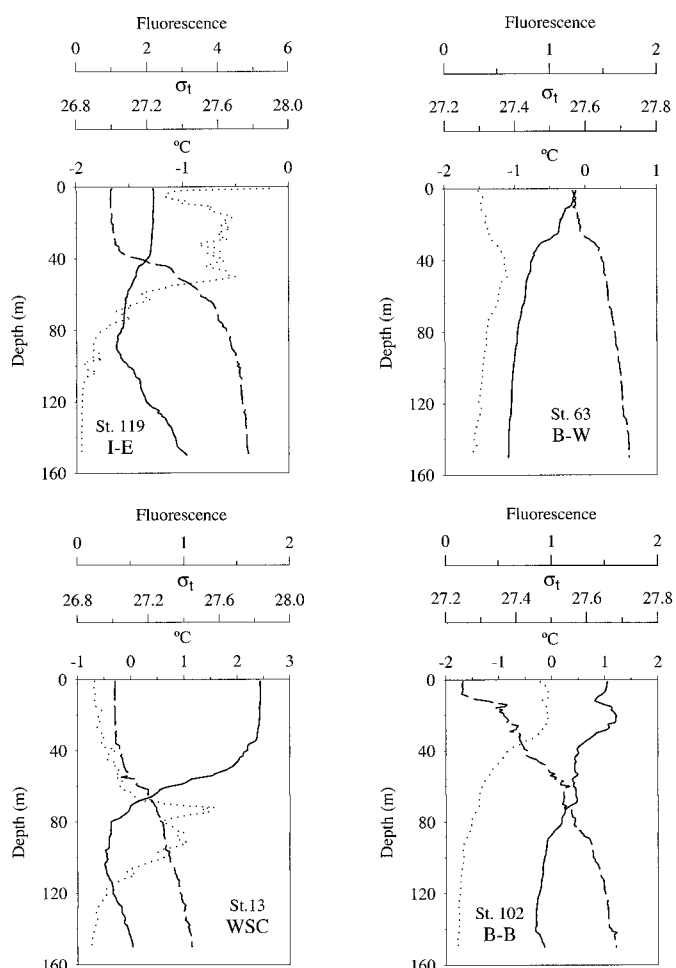


Fig. 2. CTD profiles of temperature (continuous line), density (broken line), and fluorescence (dotted line) at representative stations of the four water bodies in the sampled region.

$$E_{umI\text{PAR}} = \frac{1}{Z_{umI}} \int_0^{Z_{umI}} \overline{E_0} \exp(-K_{PAR}Z) dz \quad (2)$$

Similarly, the mean spectral irradiance averaged for a 24-h period that phytoplankton receive in the upper mixed layer is

$$E_{umI}(\lambda) = \frac{1}{Z_{umI}} \int_0^{Z_{umI}} \overline{E_0}(\lambda) \exp(-K(\lambda)Z) dz \quad (3)$$

The depth of the upper mixed layer ( $Z_{umI}$ ) was determined assuming that a change of  $\sigma_t \geq 0.05$  over a 5-m depth interval was enough to establish the pycnocline (Mitchell and Holm-Hansen 1991). When this criterion was not clear, visual inspection of the CTD plots of salinity and fluorescence were also used.

**Chlorophyll and phytoplankton absorption coefficients**—Chlorophyll (Chl) *a* determinations were done by filtering 250 ml of seawater through 25-mm Whatman GF/F filters and the pigments extracted in 90% acetone. Chlorophyll concentrations were estimated by fluorometry using a Turner Designs fluorometer.

Seawater volumes of 1–2 liters were filtered through

Whatman GF/F filters, and the optical density spectra (350–750 nm) of concentrated particles were measured in a Kontron UVIKON 860 dual-beam spectrophotometer at 1 nm bandwidth. A wet GF/F filter was used as a blank. Optical density of nonalgal material was determined in the same filter after pigment extraction following Kishino et al. (1985). Absorbance at 750 nm was subtracted from all other wavelengths in the spectra to correct the spectral differences between sample and reference filters. The correction for pathlength amplification on the filters was carried out following Arbones et al. (1996).

**Photosynthesis–irradiance parameters (P-E)**—The P-E determinations were done in lineal incubators illuminated at the front side by Osram tungsten–halogen lamps with dichroic reflector and Deco glass cover (50 W, 12 V). Each incubator houses 14 subsamples collected in 75-ml tissue culture Corning flasks that were inoculated with  $1.85 \times 10^5$  Bq (5  $\mu\text{Ci}$ ) of  $^{14}\text{C}$ -labeled bicarbonate. The samples were maintained at sea temperature by circulating surface seawater for the 5–10-m samples and by using a Neslab digital temperature controller for the subsurface samples. The photosynthetic available radiation ( $E_{PAR}$ ) at the position of each incubation bottle was measured using a Li-Cor cosine sensor LI-190SA. The flask at the end of the incubator was covered with aluminum foil and used to measure dark fixation. After 2–3 h of incubation, the suspended material was filtered through 25-mm glass fiber filters (Whatman GF/F) at a vacuum pressure of <20 cm Hg. The filters were exposed to concentrated HCl fumes for 12 h and dpm were determined with liquid scintillation counter (Beckman) using the external standard and the channel ratio methods to correct for quenching.

The broadband P-E parameters, chlorophyll-specific light-saturated rates of photosynthesis  $P_m^B$  (mg C mg Chl $^{-1}$  h $^{-1}$ ), and the light-limited slope  $\alpha^B$  (mg C [mg Chl] $^{-1}$  h $^{-1}$  [ $\mu\text{mol m}^{-2} \text{s}^{-1}$ ] $^{-1}$ ) were estimated by fitting the data to the model of Webb et al. (1974) because photoinhibition was not experienced using the irradiance range of 1–900  $\mu\text{mol m}^{-2} \text{s}^{-1}$ :

$$P_z^B = P_m^B [1 - \exp(-\alpha^B \cdot E_{PAR} / P_m^B)] \quad (4)$$

where  $P_z^B$  is the chlorophyll-specific rate of photosynthesis (mg C mg Chl $^{-1}$  h $^{-1}$ ) at each given depth.

The spectral quality of the incident light did not change along the incubators and therefore the spectral irradiance  $E_q(\lambda)$  at each location in the incubators was deduced from the relative mean spectrum of the tungsten–halogen lamps  $E_{rel}(\lambda)$ :

$$E_{rel}(\lambda) = E(\lambda) / \int_{\lambda} E(\lambda) d\lambda \quad (5)$$

multiplied by the corresponding photosynthetic available radiation ( $E_{PAR}$ ) at each location.

The photosynthetic active radiation absorbed by phytoplankton ( $E_{PUR}$  [ $\mu\text{mol m}^{-3} \text{s}^{-1}$ ]) at each position in the incubators was estimated according to Dubinsky (1980):

$$E_{PUR} = \int_{400}^{700} a_{ph}(\lambda) \cdot E_q(\lambda) d(\lambda) \quad (6)$$

where  $a_{ph}(\lambda)$  is the phytoplankton spectral absorption coefficient.

The maximum quantum yield of carbon fixation ( $\phi_m$  mol C fixed [mol photons] $^{-1}$  absorbed) was determined by fitting the photosynthetic rates  $P$  (mg C  $m^{-3} h^{-1}$ ) to the photosynthetic radiation absorbed by phytoplankton ( $E_{PUR}$  [ $\mu\text{mol} m^{-3} s^{-1}$ ]):

$$P_z = P_m [1 - \exp(-\phi'_m \cdot E_{PUR}/P_m)] \quad (7)$$

where  $\phi_m = 0.0231 \cdot \phi'_m$ . The factor converts milligrams of carbon to moles,  $\mu\text{mol}$  of photons to moles, and hours to seconds. Because maximum photosynthetic rate is wavelength independent (Pickett and Myers 1966) then  $P_m/\text{Chl} = P_m^B$ .

A light-saturation parameter for absorbed radiation by phytoplankton ( $E_{kPUR} = P_m/\phi'_m$  [ $\mu\text{mol} m^{-3} s^{-1}$ ]) can be defined from Eq. 7, which is analogous to the saturation parameter ( $E_{kPAR}$  [ $\mu\text{mol} m^{-2} s^{-1}$ ]) for PAR irradiance.

Alternatively, maximum quantum yield can be approximated from  $\alpha^B$  and the spectrally averaged, chlorophyll-specific, absorption coefficient of phytoplankton,  $a_{ph}^*$ :

$$\phi_m = 0.0231 \cdot \alpha^B / a_{ph}^* \quad (8)$$

There are advantages in using Eq. 7 in estimating  $\phi_m$ . The light-limited slope,  $\alpha^B$ , in Eq. 8 is affected by bias caused by the spectral shape of tungsten-halogen lamps that should therefore be corrected for (Kyewalyanga et al. 1997), while Eq. 7 corrects for this spectral artifact directly.

## Results

**Hydrographic regions and phytoplankton composition**—The hydrography of the area has already been described in detail by Figueiras et al. (1998) and is summarized in Fig. 1. Briefly, three hydrographic features were found in the zone. Melting waters associated with the ice edge were observed at the southeastern part of the sampling area, while the Weddell–Scotia Confluence was situated north of Elephant Island. The front separating Bellingshausen surface waters from those with Weddell influence was located in the northern part of the Bransfield Strait. These three hydrographic features delimited four regions: Bransfield waters influenced by the Bellingshausen Sea (B-B), Bransfield waters with influence from the Weddell Sea (B-W), Weddell–Scotia Confluence waters (WSC), and Weddell waters modified by melting ice (I-E). The main characteristics of the water column in each of the four hydrographic regions are shown in Fig. 2. The melted waters at the I-E region showed an upper mixed layer of 40 m depth where chlorophyll concentration was high. The B-W waters were much more homogeneous, while in the WSC region a subsurface chlorophyll maxima was associated with the bottom of the thermocline. The B-B waters had a vertical structure similar to that of the I-E region but with a shallower upper mixed layer and warmer waters. As a consequence of these water column structures, the integrated chlorophyll (Fig. 3) showed a pattern of high chlorophyll concentrations in the I-E waters and between King George Island and Elephant Island, in waters associated with the northern part of the front where relatively strong stratification occurs (Fig. 1). WSC and B-

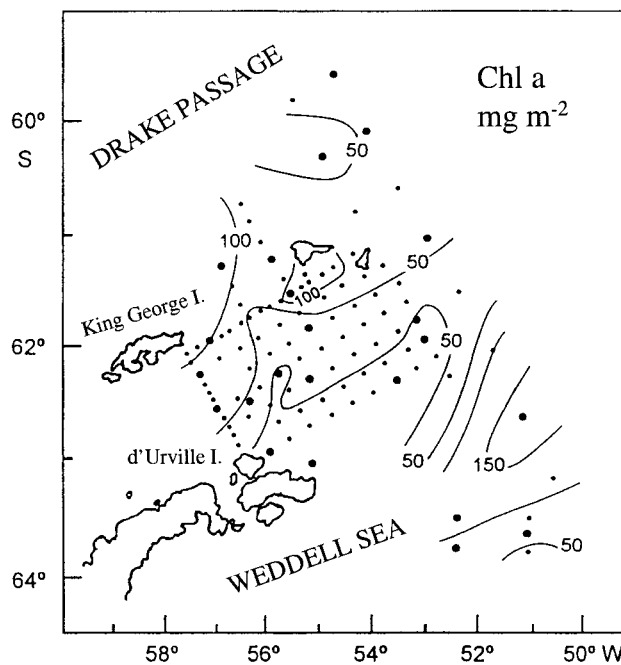


Fig. 3. Distribution of integrated Chl  $a$  concentration (mg Chl  $m^{-2}$ ) in the upper 100 m of the water column.

W waters showed integrated chlorophyll concentrations well below 50  $mg m^{-2}$ .

Diatoms dominated the WSC and I-E waters. *Rhizosolenia styliformis* was the most abundant species in the WSC waters, while *Corethron criophilum* and *Fragilariopsis* spp. dominated in the I-E waters and the Prymnesiophyceae *Phaeocystis* spp. was also abundant. The Prasinophyceae *Pyramimonas* and the Cryptophyceae *Cryptomonas* were found in the B-W waters. Diatoms, small dinoflagellates, *Cryptomonas*, and *Pyramimonas* were the main phytoplankton groups in the B-B waters. The dominant diatoms were *Pseudonitzschia* spp. and to a lesser extent *C. criophilum* (Estrada et al. unpubl.).

**Photosynthesis broadband parameters**—Table 1 shows the mean and standard deviation of the photosynthetic parameters in each hydrographic region. Data were fitted to the PE model with a coefficient of determination  $\geq 0.92$ . The actual data are given in Figueiras et al. (1998). The range of the broadband photosynthetic parameters ( $P_m^B$ ,  $\alpha^B$ , and  $E_{kPAR}$ ) was similar to that found in the area previously (e.g., Jacques 1983; Figueiras et al. 1994; Boyd et al. 1995). The relatively low values of the broadband light saturation parameter  $E_{kPAR}$  indicate low-light adaptation of the phytoplankton. There were no differences in  $P_m^B$  and  $\alpha^B$  between surface and subsurface layers ( $t$ -test for two samples;  $P_m^B$ ,  $P = 0.2$ ;  $\alpha^B$ ,  $P = 0.6$ ). Figueiras et al. (1998) showed that the maximum photosynthetic rate ( $P_m^B$ ) and the broadband initial slope ( $\alpha^B$ ) from WSC waters were statistically different from those of the other three water bodies ( $P_m^B$ ,  $0.042 > P > 0.01$ ;  $\alpha^B$ ,  $0.015 > P > 0.0003$ ). Conversely, the broadband light saturation parameter ( $E_{kPAR}$ ) was not statistically different among the four water bodies ( $0.88 > P > 0.46$ ). The same

Table 1. Mean and standard deviations of the photosynthetic parameters and light regime in the water column on each of the 4 hydrographic regions found in the area.\*

Bio-optical variable	BB	BW	IE	WSC
$P_m^B$	1.60 ± 0.42	1.41 ± 0.36	1.63 ± 0.65	0.79 ± 0.52
$\alpha^B$	0.019 ± 0.004	0.017 ± 0.008	0.022 ± 0.012	0.007 ± 0.003
$E_{kPAR}$	84 ± 22	88 ± 22	82 ± 21	100 ± 42
$E_{umIPAR}^\ddagger$	67 ± 38	44 ± 40	79 ± 26	67 ± 60
$a_{ph}$	0.018 ± 0.009	0.0084 ± 0.0025	0.0165 ± 0.0062	0.0083 ± 0.0054
$\phi_m$	0.066 ± 0.024	0.064 ± 0.035	0.062 ± 0.051	0.031 ± 0.018
$E_{kPUR}$	1.02 ± 0.52	0.49 ± 0.21	0.90 ± 0.48	0.40 ± 0.32
$E_{umIPUR}$	1.88 ± 0.95	0.63 ± 0.55	1.08 ± 0.44	0.47 ± 0.15

\* BB, Bransfield–Bellingshausen waters; BW, Bransfield–Weddell waters; IE, ice edge waters; WSC, Weddell Scotia Confluence waters.

† Units for the bio-optical variables are as follows:  $P_m^B$ : mg C (mg Chl)<sup>-1</sup> h<sup>-1</sup>;  $\alpha^B$ : mg C (mg Chl)<sup>-1</sup> h<sup>-1</sup> ( $\mu\text{mol m}^{-2} \text{s}^{-1}$ );  $E_{kPAR}$  and  $E_{umIPAR}$ :  $\mu\text{mol m}^{-2} \text{s}^{-1}$ ;  $a_{ph}$ : m<sup>-1</sup>;  $\phi_m$ : mol C (mol photons)<sup>-1</sup>;  $E_{kPUR}$  and  $E_{umIPUR}$ :  $\mu\text{mol m}^{-3} \text{s}^{-1}$ .

‡ When considering only those stations with an upper mixed layer of less than 150 m, the  $E_{umIPAR}$  value for BW was 83 ± 23.

authors showed that the mean irradiance in the upper mixed layer ( $E_{umIPAR}$ ) was not statistically different from the mean light saturation parameter ( $E_{kPAR}$ ), and these differences were even less when stations with an upper mixed layer  $\geq 150$  m were not considered (*t*-test NS,  $P = 0.83$ , see also Table 1). Mean  $E_{umIPAR}$  values, however, were slightly lower than  $E_{kPAR}$  values in the four hydrographic regions (Table 1). Furthermore,  $\alpha^B$  were not corrected for the bias caused by the tungsten–halogen lamps and, therefore, are approximately 15–40% higher than light-limited slopes calculated with spectral correction (Kyewalyanga et al. 1997). It could be argued, therefore, that  $E_{kPAR}$  values should be higher than those observed in Table 1, and consequently, phytoplankton might have been limited by PAR. Small differences in PAR light intensity, therefore, have important consequences for carbon fixation because a small increase or decrease in light level can shift phytoplankton carbon uptake from the light-limited to the light-saturated region of the photosynthesis–irradiance curve and vice versa. This would cause high dissimilarities in the rates of primary production given the high light-limited slopes of the P-E curves.

**Maximum quantum yields**—Maximum quantum yields of carbon fixation ( $\phi_m$ , mol C [mol photons]<sup>-1</sup>) in the area varied by a factor of 9, ranging from nearly 10% to 90% of the theoretical maximum of 0.125 mol C (mol photons)<sup>-1</sup> (Fig. 4). The distributions of  $\phi_m$  at surface and subsurface depths were very similar. In fact a *t*-test for two samples showed no significant differences between surface and subsurface maximum quantum yield ( $\phi_{max} = 0.06 \pm 0.036$ ,  $P = 0.95$ ). High similarities between  $\phi_m$  at both layers were found in I-E, B-W, and WSC regions ( $0.75 > P > 0.57$ ), whereas B-B waters did not show such high similarity ( $P = 0.06$ ), possibly due to the stronger influence of the surface, relative to the subsurface, of WSC waters on the B-B region (see Figs. 1, 5). The mean value of 0.06 mol C (mol photons)<sup>-1</sup> can be considered typical of nutrient-replete phytoplankton (Cleveland et al. 1989; Platt et al. 1992). Highest values ( $>0.06$  mol C [mol photons]<sup>-1</sup>) were found at the continental shelf near d’Urville Island, at the I-E stations closest to the pack ice, and at the frontal structure (B-B waters) located between King George Island and Elephant Island. The low-

est  $\phi_m$  values ( $<0.03$  mol C [mol photons]<sup>-1</sup>) were at the WSC stations, while the central part of the study area occupied by B-W waters and I-E waters, with a higher influence of Weddell Sea had intermediate values ( $0.03 < \phi_m < 0.06$ ). The variability of  $\phi_m$  in these Antarctic regions was similar to that reported previously for other waters with strongly different characteristics, such as the California Current (Sosik 1996), Southern California Bight (Schofield et al. 1993), and the Sargasso Sea (Cleveland et al. 1989). These authors have suggested that environmental conditions such as light level, temperature, and nutrient availability can affect the maximum quantum yield. We did not find any significant correlation, neither using multiple nor simple linear regression analysis, with these environmental variables, probably because the mean irradiance in the upper mixed layer ( $E_{umIPAR}$ , Table 1) and the water column temperature (Fig. 2) were not extremely different between the four water bodies. Major macronutrients were also not limiting (data not shown), and phytoplankton species did not differ greatly. What could therefore be the possible causes for the lower average  $\phi_m$  in WSC waters? The mean  $\phi_m$  of WSC (0.03 mol C [mol photons]<sup>-1</sup>, Table 1) was significantly lower than that of the other three water bodies (*t*-test,  $0.013 < P < 0.03$ ). De Baar et al. (1995) found that iron limitation seems to be important at the WSC region. The mean  $\phi_m$  value of WSC waters (Table 1) is 25% of the theoretical maximum and is close to the value reported by Lindley et al. (1995) for iron-limited equatorial Pacific waters with no nitrate limitation. Conversely, the mean  $\phi_m$  values for the other three water bodies ( $>0.06$  mol C mol photons<sup>-1</sup>, Table 1) are compatible with no macro- and micronutrient limitation of photosynthesis (Cleveland et al. 1989; Platt et al. 1992; Lindley et al. 1995). This observation requires further studies on the photophysiology of phytoplankton in micronutrient-limited waters of the Southern Ocean.

**Light regime in the water column**—Variability of the phytoplankton absorption spectra was high in both surface and subsurface samples (Fig. 5), but in spite of this variability there were no differences in the mean absorption coefficient between the surface and subsurface within each hydrographic region ( $0.5 > P > 0.3$ ). Consequently, the mean absorp-

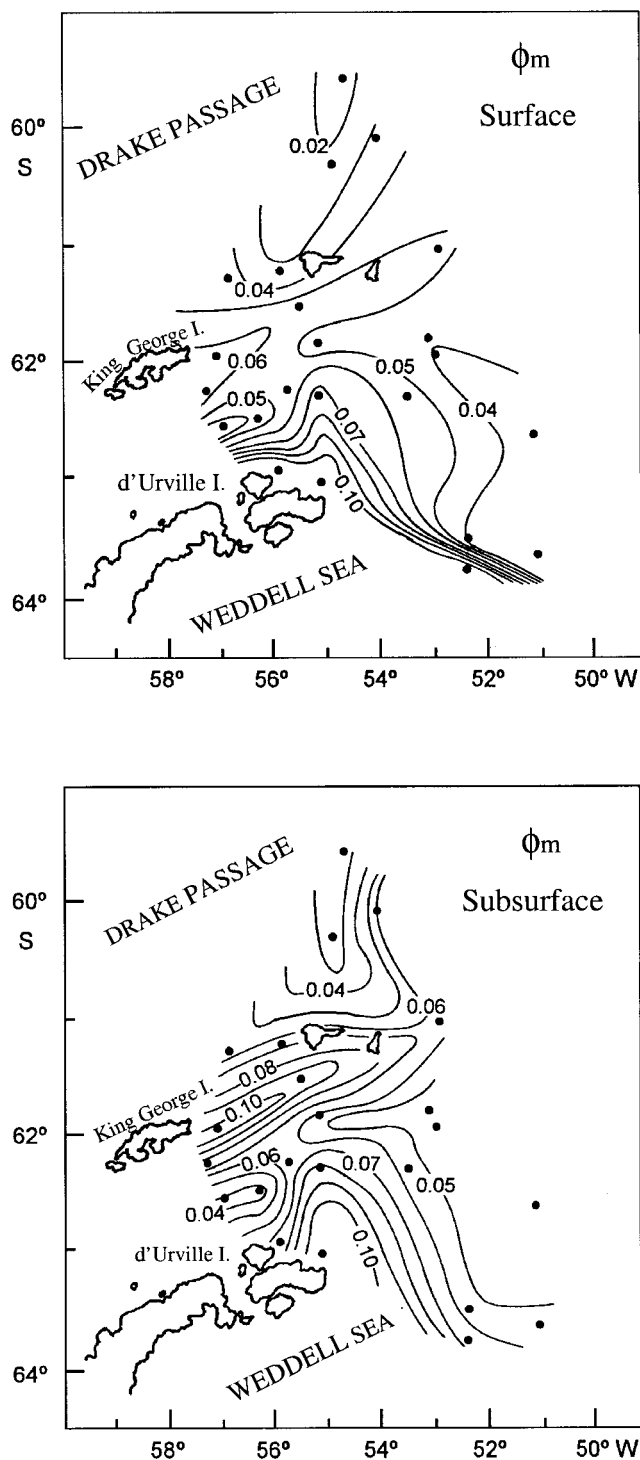


Fig. 4. Distribution of maximum quantum yield ( $\phi_m$ , mol C [mol photons] $^{-1}$ ) at the surface (5–10 m) and subsurface (30–70 m) waters.

tion coefficients in the two layers were not statistically different, as revealed by a *t*-test for two samples ( $\bar{a}_{ph} = 0.012 \pm 0.007 \text{ m}^{-1}$ ,  $P = 0.4$ ). Because there were no differences between surface and subsurface samples, they were pooled and differences between the four hydrographic regions were

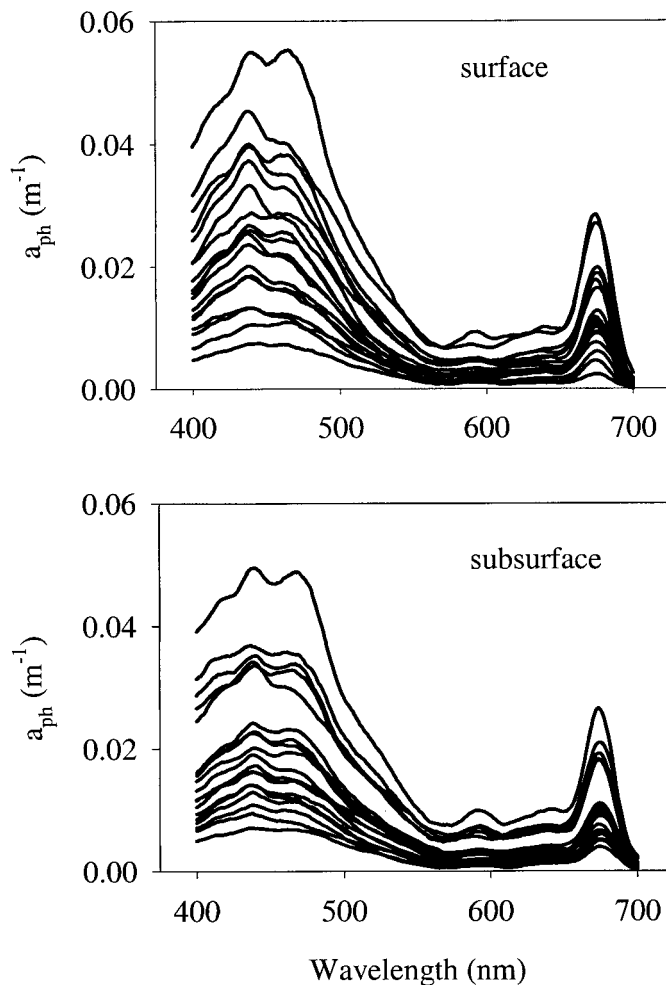


Fig. 5. Phytoplankton absorption spectra at the surface (5–10 m) and subsurface (30–70 m) waters.

analyzed. Significant differences were found between the mean absorption coefficient of B-B, B-W, and WSC ( $0.012 < P < 0.02$ ) and I-E, WSC, and B-W ( $0.007 < P < 0.02$ ) (Table 1). The mean absorption coefficients of I-E and B-B were not statistically different (*t*-test,  $P = 0.63$ ) as well as those from B-W and WSC (*t*-test,  $P = 0.96$ ). In accordance with the chlorophyll distribution,  $\bar{a}_{ph}$  was higher in those regions (B-B and I-E, Table 1) with higher depth-integrated chlorophyll concentration (Fig. 3).

As there were no significant differences in  $\bar{a}_{ph}$  between surface and subsurface layers, this enabled us to estimate the mean irradiance absorbed by phytoplankton in the upper mixed layer  $E_{umIPAR}$  (Table 1) using the equation:

$$E_{umIPUR} = \int_{400}^{700} \bar{a}_{ph}(\lambda) \cdot E_{uml}(\lambda) d(\lambda) \quad (9)$$

where  $\bar{a}_{ph}(\lambda)$  is the average of the two phytoplankton absorption spectra in the water column.

The spectral light saturation parameter ( $E_{kPUR}$ ,  $\mu\text{mol m}^{-3} \text{ s}^{-1}$ ), unlike the broadband light saturation parameter ( $E_{kPAR}$ ,  $\mu\text{mol m}^{-2} \text{ s}^{-1}$ ), showed significant differences among the hydrographic regions (Table 1). The B-B waters had a higher

$E_{kPUR}$  than those from B-W and WSC ( $t$ -test,  $0.018 < P < 0.016$ ), while  $E_{kPUR}$  from B-W and WSC were not significantly different ( $t$ -test NS,  $P = 0.59$ ). I-E  $E_{kPUR}$  was more similar to B-B  $E_{kPUR}$  ( $P = 0.66$ ) than to those from B-W and WSC ( $P = 0.06$ ). A similar pattern occurred for the mean spectral irradiance absorbed by phytoplankton in the upper mixed layer ( $E_{umlPUR}$ , Table 1); B-W and WSC were not significantly different ( $P = 0.40$ ), and  $E_{umlPUR}$  from B-B was significantly higher than those from B-W and WSC ( $0.03 < P < 0.04$ ). The differences between hydrographic regions could be attributed to differences in phytoplankton absorption spectra, because  $\overline{E_{kPAR}}$  and  $E_{umlPAR}$  were similar in the four regions. In fact  $a_{ph}$  shows a similar pattern to that of  $E_{kPUR}$  and  $E_{umlPUR}$  (Table 1). No differences were found between  $E_{kPUR}$  and  $E_{umlPUR}$  when all samples were pooled together ( $\overline{E_{kPUR}} = 0.67 \pm 0.43$ ;  $\overline{E_{umlPUR}} = 0.96 \pm 0.78$ ;  $P = 0.11$ ) or within each respective region (Table 1;  $0.12 < P < 0.70$ ). The similarity between  $E_{kPUR}$  and  $\overline{E_{umlPUR}}$  was higher in WSC waters ( $P = 0.70$ ) and lower in B-B waters ( $P = 0.12$ ). By comparison with  $E_{kPAR}$  and  $E_{umlPAR}$ , the mean spectral irradiance absorbed by phytoplankton in the upper mixed layer ( $E_{umlPUR}$ ) was always slightly higher than the spectral light saturation parameter ( $E_{kPUR}$ ), suggesting that photosynthesis was not light limited. This supports the hypothesis previously proposed by Figueiras et al. (1994, 1998) using  $E_{kPAR}$  and  $E_{umlPAR}$  that phytoplankton carbon fixation in well-mixed Antarctic waters occurs at a maximum rate.

*Evidence of no light limitation using water column quantum yield*—Another way to check if photosynthesis is light saturated or light limited is by comparing maximum versus in situ quantum yields. According to the definition of quantum yield (mol C fixed per mol photons absorbed), this will be maximum under light-limited conditions because the efficiency in using the light absorbed in carbon fixation is maximal. Thus, if light limitation of photosynthesis occurs, the in situ or realized quantum yield will be equal to maximum quantum yield, because photosynthesis is taking place in the light-limited region of the P-E curve. Conversely, the in situ quantum yield will be lower than the maximum quantum yield when photosynthesis is light saturated.

The mean water column operational quantum yields  $\overline{\phi}$  were estimated as follows:

$$\overline{\phi} = \frac{1}{Z} \int_0^z P/E_{PUR} dz \quad (10)$$

where  $P$  (see Eq. 11 in the following section) and  $E_{PUR}$  are expressed in units of mol C m<sup>-3</sup> d<sup>-1</sup> and mol photons m<sup>-3</sup> d<sup>-1</sup>, respectively, and were calculated for the photic layer and for the upper mixed layer (Fig. 6). The mean realized quantum yield in the photic layer (0.03 mol C [mol photons]<sup>-1</sup>) was not significantly different ( $P = 0.18$ ) from that in the upper mixed layer (0.027 mol C [mol photons]<sup>-1</sup>) and both were well below ( $P < 0.001$ ) the corresponding maximum quantum yields (Fig. 7). These operational quantum yields that are significantly lower ( $P < 0.001$ ) than the mean  $\overline{\phi}_m = 0.06$ , confirm that carbon fixation of Antarctic phytoplankton is taking place at saturating light, such as it had been suggested previously from white-light photosynthetic parameters (Figueiras et al. 1994, 1998) and in the previous

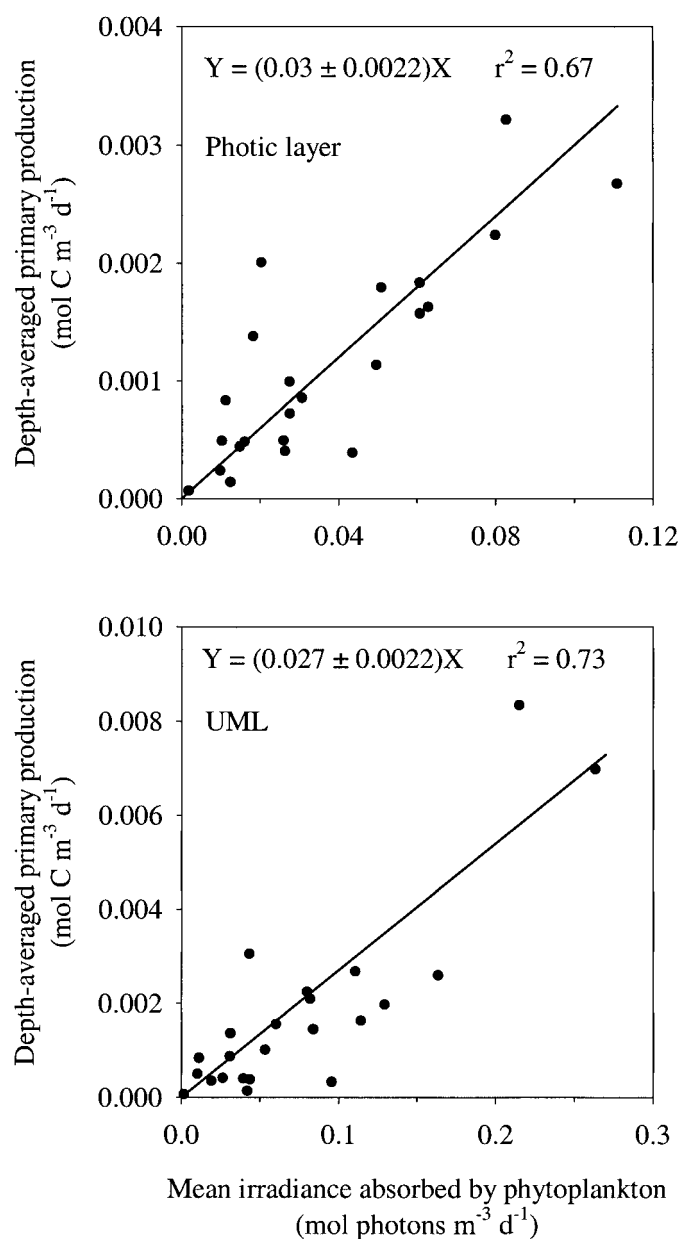


Fig. 6. Depth-averaged primary production versus mean irradiance absorbed by phytoplankton in the photic layer and in the upper mixed layer (UML). Equations inside are those for model II of linear regressions. The slopes shown represent an estimate of the mean realized quantum yield in each respective water column ( $P < 0.001$ ).

section comparing  $E_{kPUR}$  and  $E_{umlPUR}$ . If this were not the case, the operational quantum yield would not be significantly lower than the maximum quantum yield. The significant linear relationship found between the mean primary production in the water column and the mean irradiance absorbed by phytoplankton (Fig. 6) might suggest light limitation. However, the fact that the slope of the regression ( $\overline{\phi} = 0.03$ ) is significantly lower than the average maximum quantum yield ( $\overline{\phi}_m = 0.06$ ), indicates no light limitation. Linear relationship between primary production and light absorbed

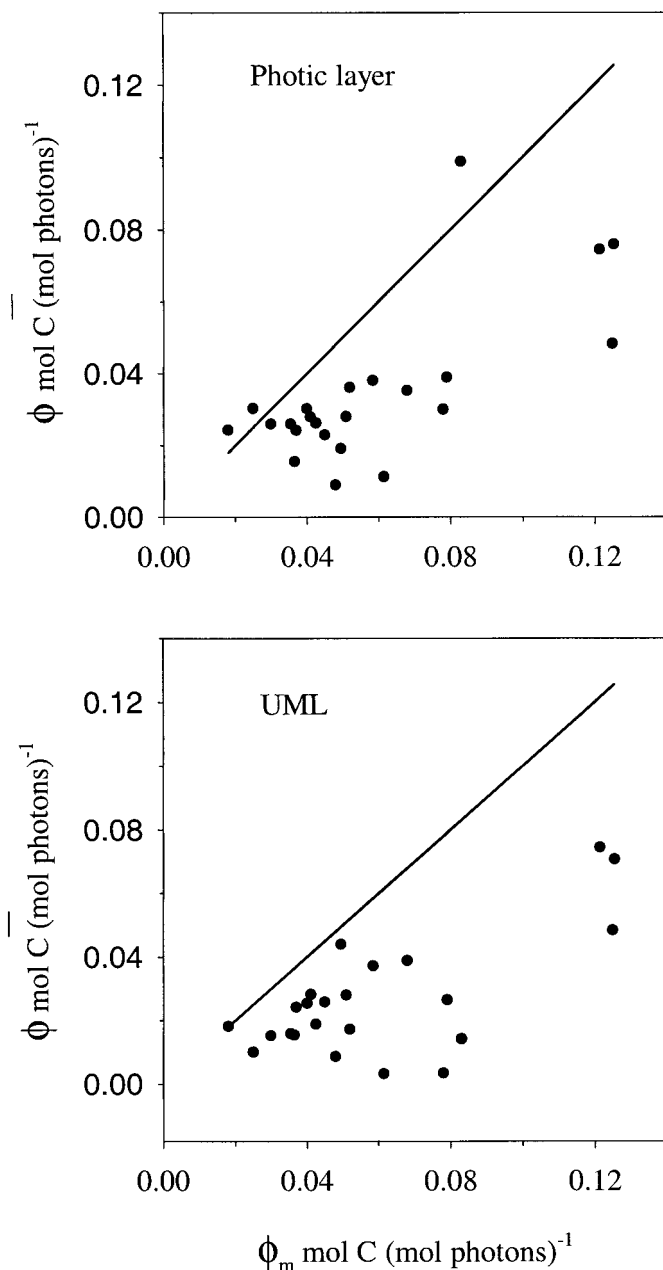


Fig. 7. Depth-averaged operational quantum yield versus average maximum quantum yield in the photic layers and in the upper mixed layers (UML). Solid lines correspond to 1:1 relationships.

by phytoplankton with no light limitation is possible when covariation between  $E_{kPUR}$  and  $E_{umIPUR}$  exists, while  $\phi_m$  is constant and carbon uptake is occurring at saturating light levels close to  $E_{kPUR}$ .

**Primary production**—Depth-integrated primary production at each station ( $P$ ) was calculated as follows:

$$P = D \int_0^z \text{Chl} \cdot P_m^B \cdot [1 - \exp(-E_{PUR}/E_{kPUR})] dz \quad (11)$$

where the daylength  $D$  is 24 h because irradiance was av-

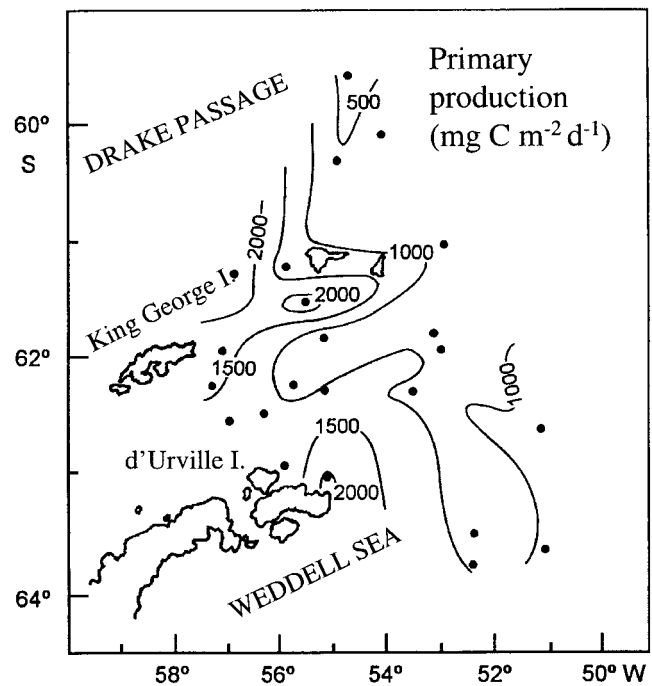


Fig. 8. Distribution of integrated primary production ( $\text{mg C m}^{-2} \text{d}^{-1}$ ).

eraged for this period. The integration depth was that of the photic layer in the stations where the depth of 1% of light was deeper than the upper mixed layer ( $Z_{uml}$ ) and was  $Z_{uml}$  in the stations where the photic layer was shallower than the upper mixed layer.

Primary production in the sampling area was highly variable (Fig. 8) with values typical of oligotrophic waters, of the most productive upwelling systems and of Antarctic regions with high chlorophyll concentrations (Boyd et al. 1995). The distribution of integrated primary production reflected the existing hydrographic structures in the area. The highest values ( $>2,000 \text{ mg C m}^{-2} \text{d}^{-1}$ ) were found in the stratified waters under the influence of Bellinghousen Sea and in the coastal waters close to d'Urville Island, where chlorophyll concentration and maximum quantum yields were relatively high (Figs. 3, 4). These high primary production values are similar to those observed over the continental shelf in the Gerlache Strait (Mandelli and Burkholder 1966; Holm-Hansen and Mitchell 1991). Waters from WSC that had the lowest maximum quantum yield of the sampled region (Fig. 4) showed also the lowest integrated primary production values (Fig. 8).

Integrated primary production was computed considering PAR irradiance and compared with values calculated from spectral irradiance and light absorbed by phytoplankton (Eq. 11). A good correlation was found between both estimates (Fig. 9), but primary production was 24% lower using the PAR model than the PUR model. This difference between both estimates must be attributed to the fact that light limitation may appear to occur when PAR irradiance is used for estimating the photosynthetic parameters, while the use of spectral irradiance shows that the photosynthetic response is light saturated (see text above and Table 1).

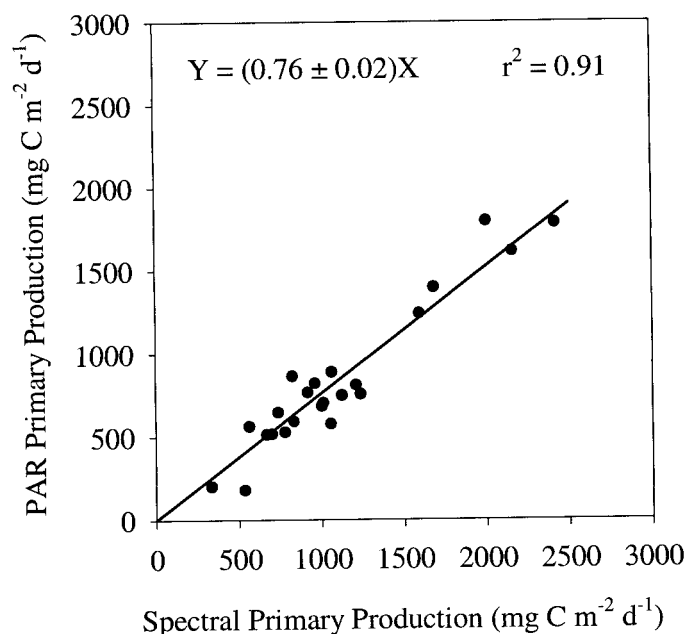


Fig. 9. Comparison between integrated primary production ( $\text{mg C m}^{-2} \text{d}^{-1}$ ) estimated using PAR irradiance and spectral irradiance in the water column. The equation inside is for model II of the linear regression.

## Conclusions

The bio-optical parameters determined in the eastern basin of the Bransfield Strait (Antarctica) indicate that phytoplankton photosynthesis in the upper mixed layer of these waters was not light limited. This is deduced from the similarity between the light saturation parameters of both spectral and broadband photosynthesis–irradiance relationships ( $E_{KPAR}$ ,  $E_{KPAR}$ ) and the corresponding mean irradiance in the upper mixed layer ( $E_{umIPUR}$ ,  $E_{umIPAR}$ ). Spectral photosynthesis–irradiance relationships showed no light limitation, while broadband relationships indicated slight light limitation. Because photosynthesis takes place at light levels close to the light saturation parameter, primary production computed using broadband relationships can significantly underestimate the depth-integrated primary production. In this study, it was as much as 24% and indicated that these differences may have important consequences in modeling carbon flow in the Southern Ocean. It is suggested, therefore, that primary production should be computed from spectral photosynthesis–irradiance relationships. The operational quantum yields of the water column also support the conclusion that carbon uptake was not light limited.

## References

- ARBONES, B., F. G. FIGUEIRAS, AND M. ZAPATA. 1996. Determination of phytoplankton absorption coefficient in natural seawater samples: Evidence of a unique equation to correct the pathlength amplification on glass-fiber filters. *Mar. Ecol. Prog. Ser.* **137**: 293–304.
- AUSTIN, R. W. 1974. Inherent spectral radiance signatures of the ocean surface, p. 1–20. *In* Ocean color analysis, SIO reference 74-10. Univ. of California, San Diego.
- BOYD, P. W., C. ROBINSON, G. SAVIDGE, AND P. J. LE B. WILLIAMS. 1995. Water column and se-ice primary production during austral spring in the Bellingshausen sea. *Deep-Sea Res. II* **42**: 1177–1200.
- CLEVELAND, J. S., M. J. PERRY, D. A. KIEFER, AND M. C. TALBOT. 1989. Maximum quantum yield of photosynthesis in the northwestern Sargasso Sea. *J. Mar. Res.* **47**: 869–889.
- DUBINSKY, Z. 1980. Light utilization efficiency in natural phytoplankton communities, p. 83–97. *In* P. J. Falkowski [ed.], Primary productivity in the sea. Plenum.
- DE BAAR, H. J. W., J. T. M. DE JONG, D. C. E. BAKKER, B. M. LÖSCHER, C. VETH, U. BATHMANN, AND V. SMETACEK. 1995. Importance of iron for plankton blooms and carbon dioxide drawdown in the Southern Ocean. *Nature* **373**: 412–415.
- EL-SAYED, S. Z. 1970. On the productivity of the Southern Ocean, p. 119–135. *In* N. W. Holgate [ed.], Antarctic ecology. Academic.
- . 1987. Biological productivity of Antarctic waters: Present paradoxes and emerging paradigms, p. 1–21. *In* S. Z. El-Sayed and A. P. Tomo [eds.], Antarctic aquatic biology. SCAR.
- FIGUEIRAS, F. G., M. ESTRADA, O. LÓPEZ, AND B. ARBONES. 1998. Photosynthetic parameters and primary production in the Bransfield Strait: Relationships with mesoscale hydrographic structures. *J. Mar. Syst.* **17**: 129–141.
- , F. F. PÉREZ, Y. PAZOS, AND A. F. RÍOS. 1994. Light and productivity of Antarctic phytoplankton during austral summer in an ice edge region in the Weddell–Scotia Sea. *J. Plankton Res.* **16**: 233–253.
- GARCÍA, M. A., AND OTHERS. 1994. Mesoscale variability in the Bransfield Strait region (Antarctica) during austral summer. *Ann. Geophys.* **12**: 856–867.
- HELBLING, E. W., V. E. VILLAFANE, AND O. HOLM-HANSEN. 1995. Variability of phytoplankton distribution and primary production around Elephant Island, Antarctica, during 1990–1993. *Polar Biol.* **15**: 233–246.
- HOLM-HANSEN, O., S. Z. EL-SAYED, G. A. FRANCESCHINI, AND R. L. CUHEL. 1977. Primary production and the factors controlling phytoplankton growth in the Southern Ocean, p. 11–50. *In* Adaptations within Antarctic ecosystems: Proceedings of the third SCAR Symposium on Antarctic biology. Smithsonian Institution.
- , AND B. G. MITCHELL. 1991. Spatial and temporal distribution of phytoplankton and primary production in the western Bransfield Strait region. *Deep-Sea Res.* **38**: 961–980.
- JACQUES, G. 1983. Some ecophysiological aspects of Antarctic phytoplankton. *Polar Biol.* **2**: 27–33.
- KIRK, J. T. O. 1983. Light and photosynthesis in aquatic ecosystems. Cambridge Univ. Press.
- KISHINO, M., N. TAKAHASHI, N. OKAMI, AND S. ICHIMURA. 1985. Estimation of the spectral absorption coefficients of phytoplankton in the sea. *Bull. Mar. Sci.* **37**: 634–642.
- KYEWALYANGA, M., T. PLATT, AND S. SATHYENDRANATH. 1997. Estimation of the photosynthetic action spectrum: Implication for primary production models. *Mar. Ecol. Prog. Ser.* **146**: 207–223.
- LINDLEY, S. T., R. R. BIDIGARE, AND R. T. BARBER. 1995. Phytoplankton photosynthesis parameters along 140°W in the equatorial Pacific. *Deep-Sea Res. II* **42**: 441–463.
- MANDELLI, E. G., AND P. R. BURKHOLDER. 1966. Primary productivity in the Gerlache and Bransfield Straits of Antarctica. *J. Mar. Res.* **24**: 15–27.
- MARTIN, J. H., M. R. GORDON, AND S. E. FITZWATER. 1991. The case for iron. *Limnol. Oceanogr.* **36**: 1793–1802.
- MITCHELL, B. G., AND O. HOLM-HANSEN. 1991. Observations and

- modeling of the Antarctic phytoplankton crop in relation to mixing depth. *Deep-Sea Res. II* **38**: 981–1007.
- PICKETT, J. M., AND J. MYERS. 1966. Monochromatic light saturation curves for photosynthesis in *Chlorella*. *Plant Physiol.* **41**: 90–98.
- PLATT, T., S. SATHYENDRANATH, O. ULLOA, W. G. HARRISON, N. HOEPPFNER, AND J. GOES. 1992. Nutrient control of phytoplankton photosynthesis in the western north Atlantic. *Nature* **356**: 229–231.
- SAKSHAUG, E., AND O. HOLM-HANSEN. 1984. Factors governing pelagic production in polar oceans, p. 1–18. *In* O. Holm-Hansen, L. Bolis, and R. Gilles [eds.], *Marine phytoplankton and productivity*. Springer.
- SCHOFIELD, O., B. B. PRÉZELIN, R. R. BIDIGARE, AND R. C. SMITH. 1993. In situ photosynthetic quantum yield. Correspondence to hydrographic and optical variability in the Southern California Bight. *Mar. Ecol. Prog. Ser.* **93**: 25–37.
- SMETACEK, V., R. SCHREK, AND E. M. NÖTHIG. 1990. Seasonal and regional variation in the pelagial and its relationship to the life history cycle of krill, p. 103–114. *In* K. R. Kerry and G. Hempel [eds.], *Antarctic ecosystems. Ecological change and conservation*. Springer.
- SOSIK, H. M. 1996. Bio-optical modeling of primary production: Consequences of variability in quantum yield and specific absorption. *Mar. Ecol. Prog. Ser.* **143**: 225–238.
- WEBB, W. L., M. NEWTON, AND D. STARR. 1974. Carbon dioxide exchange of *Alnus rubra*: A mathematical model. *Oecologia* **17**: 281–291.

*Received: 30 November 1998*

*Accepted: 8 June 1999*

*Amended: 12 July 1999*